# Faraday Discussions

Accepted Manuscript


This manuscript will be presented and discussed at a forthcoming Faraday Discussion meeting. All delegates can contribute to the discussion which will be included in the final volume.

**Register now to attend!** Full details of all upcoming meetings: http://rsc.li/fd-upcoming-meetings

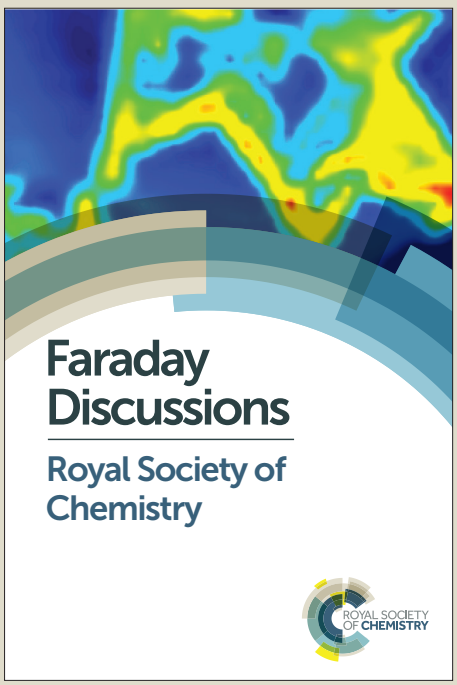


This is an *Accepted Manuscript*, which has been through the Royal Society of Chemistry peer review process and has been accepted for publication.

*Accepted Manuscripts* are published online shortly after acceptance, before technical editing, formatting and proof reading. Using this free service, authors can make their results available to the community, in citable form, before we publish the edited article. We will replace this *Accepted Manuscript* with the edited and formatted *Advance Article* as soon as it is available.

You can find more information about *Accepted Manuscripts* in the Information for Authors.

Please note that technical editing may introduce minor changes to the text and/or graphics, which may alter content. The journal's standard Terms & Conditions and the Ethical guidelines still apply. In no event shall the Royal Society of Chemistry be held responsible for any errors or omissions in this *Accepted Manuscript* or any consequences arising from the use of any information it contains.

ROYAL SOCIETY OF CHEMISTRY

www.rsc.org/faraday_d

CREATED USING THE RSC REPORT TEMPLATE (VER. 3.1) - SEE WWW.RSC.ORG/ELECTRONICFILES FOR DETAILS
Faraday Discussions
REVIEW www.rsc.org/xxxxxx | XXXXXXXX

# Computational Investigation of Hole Mobilities in Organic Semiconductors: Comparison of Single Crystal Structures and Surface Adsorbed Clusters

**Rose A. Krawczuk,[a]* Steven Tierney,[b] William Mitchell[b] and Joseph J. W. McDouall[a]**

**DOI: 10.1039/b000000x [DO NOT ALTER/DELETE THIS TEXT]**

## Abstract

We report hole mobilities obtained computationally based on both single crystal geometries and those obtained from crystal fragments optimised on a model surface. Such computational estimates can differ considerably from experimentally measured thin film mobilities. One source of this discrepancy is due to a difference in the morphology of the thin film compared with that of the crystal. Here, predictions of thin film hole mobilities based on optimised structures are given. A model surface is used to provide an inert geometric platform for the formation of an organic monolayer. The model is tested on pentacene and TIPS-pentacene for which experimental information of the surface morphology exists. The model has also been applied to four previously uninvestigated structures. Two of the compounds studied had fairly low predicted mobilities in their single crystal structures, which were vastly improved post-optimisation. This is in accord with experiment.

## 1 Introduction

Owing to their potential for low-cost manufacture, thin films of molecular organic materials have attracted interest in technologies such as organic field-effect transistors (OFETs), light-emitting diodes (OLEDs) and photovoltaics (OPVs). Molecular acenes such as pentacene exhibit relatively high field-effect mobilities, a measure of the conductivity, which has prompted the derivatisation of acene cores in order to optimise these properties.

Herein, particular emphasis is placed on OFETs, for which a wide range of differently configured devices can be created, each affecting the mobility in a specific way. Most research in this area focusses on bottom-gate bottom-contact devices due to ease of production,[1] the layout of which is shown in Fig. 1. There also exist many methods for production of thin films of molecular materials. Each method of production (e.g. physical vapour deposition, spin-coating) subtly influences the morphology of the thin film and consequently the mobility. Crystalline and polycrystalline thin films tend to have higher mobilities than their amorphous counterparts. Charge transport in polycrystalline films is hampered by boundaries between crystal grains. By changing certain conditions during deposition, for example optimising the substrate temperature, one can alter these



This journal is © The Royal Society of Chemistry [year]

Faraday Discussions Accepted Manuscript

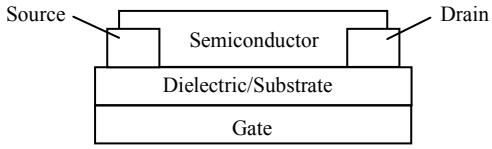


**Fig. 1** Diagram of a bottom-gate bottom-contact thin film transistor.

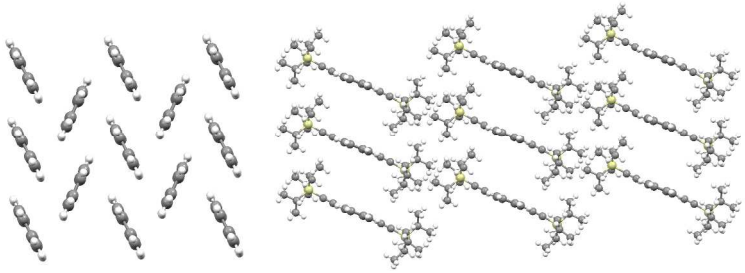

**Fig. 2** On the left, the herringbone packing motif for pentacene. On the right, the 'brick-wall packing motif for TIPS-pentacene.

types of defects, thus significantly changing the mobility of a device.

On a molecular level, the underlying packing of the molecules at the surface is also critical to the conductivity. Most charge carriers reside at the semiconductor-dielectric interface, therefore it is the first few layers of a material which define its mobility. It is the balance between molecule-molecule and molecule-substrate interactions that determine the overall structure of the thin film.[2] For instance, pentacene lies with its face down on metal surfaces due to strong molecule-substrate interactions, whereas it tends to arrange itself perpendicular to inert surfaces, for which molecule-substrate interactions are much weaker.

Since molecular organic materials generally contain some degree of anisotropy in charge transport, the orientation of the surface layers is very important. In order to achieve good charge transport, the molecules need to be orientated in such a way that their face-to-face interactions within the layers are perpendicular to the surface. It was this realisation that led John Anthony's group[3] to produce functionalised pentacene molecules, whose bulky substituents promote these types of contacts in the crystal structure. This is in contrast with pentacene molecules, which crystallise in a herringbone motif; both structures are shown in Fig. 2.

Morphology information is available for pentacene and TIPS-pentacene in their thin film phases on $SiO_2$. During the early stages of vacuum deposition, single molecules of pentacene arrange themselves face down on the $SiO_2$ surface before they begin to form clusters.[4,5] Once a cluster of pentacene molecules reaches a critical size, it is energetically more favourable for the molecules to align their long axes perpendicular to the surface. In the single crystal there is a tilt in the angle in which one pentacene unit aligns itself with another of 25°, which is 11° for the thin film phase.[6] Other studies have found that the first layer arranges itself completely upright on the surface.[7] This means that the unit cell for the bulk crystal differs from that of the thin film. It is important to note, however, that the general structural



This journal is © The Royal Society of Chemistry [year]

Faraday Discussions Accepted Manuscript

arrangement of the molecular units in their single crystal is qualitatively similar to that in the thin film. In particular, the thin film phase of TIPS-pentacene is known to coincide almost exactly with the single crystal structure.[8]

Many computational investigations focus upon the dynamics of pentacene on silica surfaces, for instance surface diffusion, molecule-substrate binding energies, defect states and thin film growth. The growth of pentacene on $SiO_2$ has been widely studied under various deposition conditions. An investigation into the nucleation of pentacene on $SiO_2$ surfaces found that the second layer nucleates when the first layer is around 80% complete, hence rationalising the observed island growth.[9] This suggests that the modelling of a monolayer on a surface could provide a good first approximation to the structure.

On a molecular scale, one study used molecular dynamics (MD) to probe the structural properties of monolayers of pentacene on $SiO_2$ in order to establish the energetic stability of competing phases.[10] In a similar investigation, MD was also used to provide a model for pentacene on an $SiO_2$ surface. The results were found to be in agreement with previous theoretical work but not experimental grazing incidence x-ray diffraction (GIXD) data. They found tilt angles for pentacene molecules on the surface of between 11.0–15.0°. The paper states that features of the $SiO_2$ surface, for instance the surface roughness, can have quite an impact on the molecular structure and hence the transport at the interface.[11]

Generally, the surface of the $SiO_2$ dielectric is functionalised in order to improve the morphology and hence the mobility of the organic semiconductor. These coatings tend to provide a better surface for dewetting of the molecular semiconductor to promote layer-by-layer growth.[12] Self-assembled monolayers (SAMs) are often used to produce more uniform interfaces with reduced surface roughness compared to $SiO_2$,[13] which has been reported to reduce the mobility of pentacene OFETs.[14] Attempts have been made to draw a correlation between the size of the pentacene grains and the mobility, but this is still unclear.[15] It has also been pointed out that a reduction in charge trapping at the $SiO_2$-semiconductor interface may be responsible for the higher mobilities on SAMs.[16] Thus there are many factors which may lead to the higher mobilities found when the dielectric surface is chemically treated.



This journal is © The Royal Society of Chemistry [year]

Faraday Discussions Accepted Manuscript

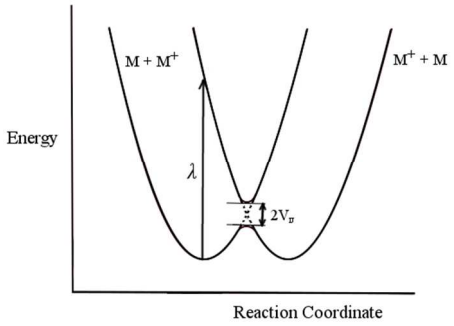


**Fig. 3** The potential energy curves for M + $M^+$ and $M^+$ + M undergoing a self-exchange reaction. When the coupling matrix element, $V_{IJ}$, is much smaller than the reorganisation energy, transfer of an electron proceeds by a 'hopping' mechanism.

## Mobility Calculations

Device-to-device reproducibility of hole mobilities tends to be poor due to the multitude of variables associated with production which affect their properties. Computationally derived mobilities can provide useful comparisons between different molecular materials. This means that mobilities for different crystals can be benchmarked against one another ignoring complications such as impurities, which can differ from one crystal to the next.

Conduction in molecular organic semiconductors proceeds by a charge hopping regime, for which Marcus's semiclassical theory of electron transfer provides a description. As depicted in Fig. 3, an electron hop is a tunnelling event that moves from the potential energy surface of the reactants, $M^+$ + M in our case, to that of the products, M + $M^+$.

The rate of charge transfer relies upon both the electronic coupling between the states and the reorganisation energy. The rate of charge transfer, $W$, within Marcus theory is given by,

$$W = \frac{V^2}{\hbar}\left(\frac{\pi}{\lambda k_B T}\right)^{\frac{1}{2}} e^{\frac{-\lambda}{4k_B T}} \quad (1)$$

where $V$ is the electronic coupling and $\lambda$ is the reorganisation energy. The electronic coupling represents the strength of interaction between the initial and final electronic states and is given by the coupling matrix element, $V_{IJ}$.

$$V_{IJ} = \left\langle \Psi_I \left| \hat{H} \right| \Psi_J \right\rangle \quad (2)$$

Where $\Psi_I$ is the electronic wavefunction for the reactant state and $\Psi_J$ is the electronic wavefunction for the product state. $V_{IJ}$ is dependent upon the distance between the molecules and their relative orientations. It is shown in reference 17 that $V_{IJ}$ is largest when two molecules interact face-to-face and falls off as one of the molecules rotates around its long axis into a face-to-edge configuration.

The internal reorganisation energy, $\lambda_{int}$, is the energy required for the reactants in their equilibrium geometry to reorganise to the geometry of the products, plus the energy for the products undergoing the analogous process. The rate of electron transfer is exponentially dependent upon the reorganisation energy; hence small



This journal is © The Royal Society of Chemistry [year]

Faraday Discussions Accepted Manuscript

reorganisation energies are critical for high rates of transfer.

In a molecular organic crystal, each molecule is surrounded by a number of others, which vary in their relative distances and orientations. There is a finite probability that the central molecule will exchange an electron with any of the surrounding molecules. Hence, there are charge transfer rates associated with each molecular path. These rates and probabilities are incorporated into the diffusion constant, $D$, which is then used to evaluate the mobility, $\mu$, via the Einstein relation.

$$\mu = \frac{e}{k_B T} D \tag{3}$$

There are two different types of charge carrier: holes and electrons. For hole [electron] transport to occur, an electron must be removed [injected] at the electrode, thus the ionisation energy [electron affinity] for the material must match the Fermi level of the electrode. During hole [electron] transport, the electron is passed between the successive HOMO [LUMO] levels of neighbouring molecules, resulting in the formation of cations [anions] during the transfer. For most organic semiconductors, the hole mobility exceeds the electron mobility by orders of magnitude.[18]

Computational studies of hole mobilities are often performed using single crystal geometries, producing results that are often in agreement with experimentally measured values obtained from single crystal devices. Complications arise, however, when this value is compared with the thin film mobility. Since it is heavily dependent upon the molecular geometry, morphological differences between the single crystal and the thin film may result in large changes in the mobility. The present investigation attempts to simulate the morphology of a molecular organic material in a monolayer in order to obtain a better estimate for the hole mobility of a thin film.

**Surface Structure**

The sole purpose of the surface in this investigation was to provide a geometric platform for formation of the organic layer. An inert surface was therefore chosen, which was unable to chemically bond to the adsorbent. The final calculations to obtain the mobility did not consider any coupling with the surface.

Whilst satisfying these requirements, it was also sensible to choose a surface for which there were data in the literature. There are many experimental and computational studies that use amorphous silica as a dielectric layer in OFETs. Additionally, it is representative of a surface before any modifications have taken place.

The structure of amorphous silica is very complicated; it has no long range order and due to the disordered distribution of ring sizes, exhibits some degree of surface roughness. For simplicity, surface roughness has been explicitly avoided in this study. Local order is provided by four-coordinate Si atoms, bridged by O. A number of silicon-oxide compounds share these short-range properties, whilst preserving long-range order. It is shown in reference 19 that a surface adapted from the sanidine feldspar mineral can be used as a simplified model of amorphous silica. The mineral is a crystalline lattice consisting of Al, Si and O atoms, with extra cations to balance the overall negative charge. All Al atoms were converted to Si atoms and the lattice



This journal is © The Royal Society of Chemistry [year]

Faraday Discussions Accepted Manuscript

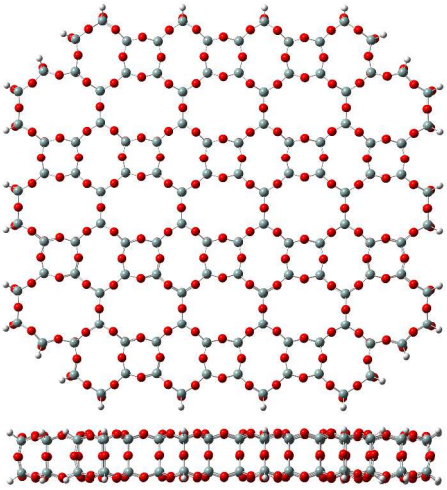

**Fig. 4** A surface slab of crystalline all-Si sanidine feldspar. Top: The view of the slab from above. Bottom: The view of the slab from the side, showing the two layers of Si atoms. This surface is incorporated into the study.

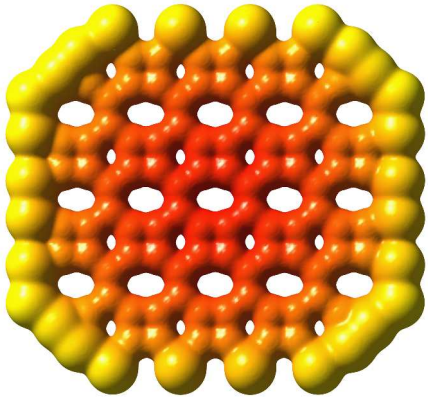

**Fig. 5** An ESP map of the surface used.

stripped of its cations. The resultant structure provides the necessary short-range order and comprises a distribution of ring sizes, with 4-, 6- and 8- member silicons. It is also important to note that silanol groups have not been taken into account in the design of this surface. Since it met all basic requirements, this structure was incorporated into the study and is shown in Fig. 4. Overall, the surface is negatively charged, as shown by the electrostatic potential (ESP) map in Fig. 5.



This journal is © The Royal Society of Chemistry [year]

Faraday Discussions Accepted Manuscript

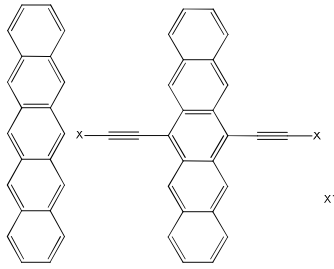

| Compound Number | X | Y |
|---|---|---|
| **3** | $SiMe_3$ | F |
| **4** | $SiMe_3$ | H |
| **5** | $SiEt_3$ | H |
| **6** | $Si(i\text{-}Pr)_3$ | H |

**1** **2** X = $Si(i\text{-}Pr)_3$ **3**, **4**, **5**, **6**

**Fig. 6** The molecules used in this study.

## Computational Details

The primary structures investigated in this study are four functionalised benzo[*k*]tetraphene molecules, **3**, **4**, **5** and **6**, see Fig. 6. These molecules were synthesised by Merck and both thin film and single-crystal devices were produced.[20] Two other molecules were chosen for the study, pentacene (**1**) and TIPS-pentacene (**2**), principally as points for correlation of known morphologies and assessment of our procedures.

Quantum chemical calculations were carried out in order to investigate the morphologies of monolayers of molecular organic materials. Optimisations were performed using both MOPAC and MOZYME,[21] at the semiempirical PM7 level, which provides reliable intermolecular interactions energies for the S22 dataset. The effects of the deposition conditions on film formation have been excluded. Hole mobilities have been calculated for the experimental single crystal structure, and also for optimised crystal fragments and monolayers at the B3LYP/6-31G(d,p) level of theory.[22]

In order to carry out the hole mobility calculation, a molecule was selected and all of its nearest neighbours were identified. Electronic couplings and reorganisation energies were evaluated for each dimer pair. The rates of electron transfer for each path were calculated, using equation 1. The diffusion constant was obtained as,

$$D = \frac{1}{2n}\sum_{i=1}^{m} r^2 P_i W_i \tag{4}$$

where $n$ is the number of dimensions, which was set to 3, $m$ is the number of nearest neighbours, $r$ is the distance between the centroids for each molecule in the dimer, $P_i$ is the probability that a certain 'hop' will take place and $W_i$ is the rate of charge transfer for each possible 'hop'. The probability is given by equation 5.

$$P_i = \frac{W_i}{\sum_i W_i} \tag{5}$$

For the reorganisation energy, the energies for the neutral and the cation molecules in their equilibrium geometries were calculated, along with the energies for the neutral molecule in the cation geometry and vice versa for the cation molecule. The overall internal reorganisation energy was evaluated using equations 6 (see Fig. 7).



This journal is © The Royal Society of Chemistry [year]

Faraday Discussions Accepted Manuscript

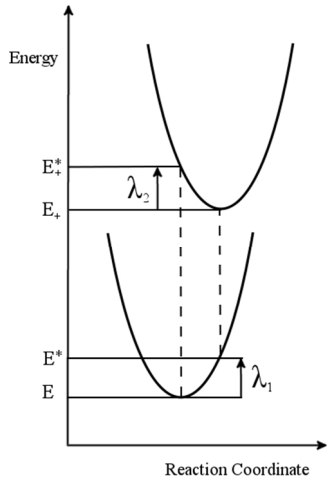


**Fig. 7** Pictorial representation of the reorganisation energy calculation.

$$\lambda_{int} = \lambda_1 + \lambda_2 \tag{6a}$$

$$\lambda_1 = \left(E^* - E\right) \quad \lambda_2 = \left(E^*_- - E_+\right) \tag{6b}$$

A program was written and interfaced to Gaussian 09[23] to evaluate the electronic couplings. This was based on the site-energy correction method, which takes into account the differences in the site energies of two molecules when they are not in the same environment.[17] The calculation assumes the HOMO and HOMO-1 levels of the dimer can be obtained by mixing of the HOMO levels of the monomers. In order to obtain the electronic coupling, the dimer Fock matrix was evaluated and transformed into the monomer basis according to equation 7.

$$\widetilde{\mathbf{F}} = \widetilde{\mathbf{S}}\widetilde{\mathbf{C}}\mathbf{E}\widetilde{\mathbf{C}}^{\mathrm{T}}\widetilde{\mathbf{S}} \tag{7}$$

Where, **E** is the diagonal matrix of orbital energies for the dimer, $\widetilde{\mathbf{S}}$ is the overlap matrix and $\widetilde{\mathbf{C}}$, the matrix of coefficients. These are block matrices formed from the **S** and **C** matrices of the monomers, as shown in equations 8 and 9.

$$\widetilde{\mathbf{C}} = \begin{pmatrix} \mathbf{C}_1 & \mathbf{0} \\ \mathbf{0} & \mathbf{C}_2 \end{pmatrix} \tag{8}$$

$$\widetilde{\mathbf{S}} = \begin{pmatrix} \mathbf{S}_1 & \mathbf{0} \\ \mathbf{0} & \mathbf{S}_2 \end{pmatrix} \tag{9}$$

The matrix $\widetilde{\mathbf{F}}$ now contains the site energies and the electronic couplings.

$$\widetilde{\mathbf{F}} = \begin{pmatrix} \boldsymbol{\varepsilon}_1 & \mathbf{V}_{12} \\ \mathbf{V}_{12} & \boldsymbol{\varepsilon}_2 \end{pmatrix} \tag{10}$$

$\widetilde{\mathbf{F}}$ is then symmetrically orthogonalised before the electronic couplings are extracted.[17]



This journal is © The Royal Society of Chemistry [year]

Faraday Discussions Accepted Manuscript

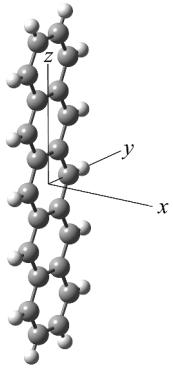


**Fig. 8** Three molecular axes of pentacene.

## 2 Results and Discussion

### Testing the Model

**Monomer Binding Energies**. The binding energies for attaching monomers of **1** and **2** over a range of locations on the surface, along each molecule's three molecular axes as depicted in Fig. 8, are shown in table 1. For **1**, the binding energy increases in the order end < edge < face down on the surface.

**Table 1** The average binding energies for monomers **1** and **2** across different sites on the surface.

| Molecule | Average Binding Energy / kJ mol$^{-1}$ | | |
|---|---|---|---|
| | End | Face | Edge |
| **1** | -15 | -69 | -36 |
| **2** | -17 | -95 | -25 |

For **2**, the difference between the end- and edge- down configurations is reduced, indicating that the greater the area of contact of the molecule with the surface, the higher the binding energy. The end- and edge- down binding energies are comparable in magnitude to two molecules interacting end-to-end or edge-to-edge. The face-down affinities are quite high, approaching the value for the binding energy of two molecules face-to-face.

As discussed previously, single molecules of **1** arrange themselves face-down on the surface of $SiO_2$ before they reach a critical cluster size. At this point they reorientate their long axes to become perpendicular with the surface. The reason for migration from a face-down to an end-down configuration can be explained in terms of binding energies. Two systems were taken; the first of which probed the evolution of the binding energy of a face-down monomer, **a**, as more molecules were added to the surface in the same orientation (Fig. 9a). The second probed an analogous system for an end-down monomer, **b** (Fig. 9b).

Fig. 10 shows the change in the binding energy of **a** compared to **b**. As before,



This journal is © The Royal Society of Chemistry [year]

Faraday Discussions Accepted Manuscript

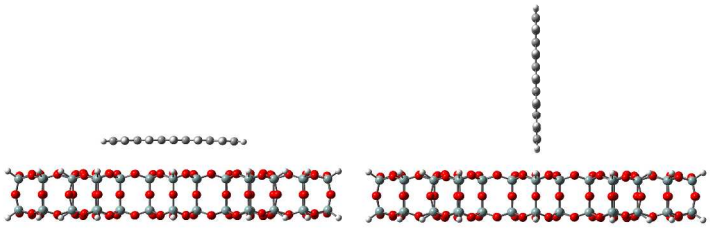

**Fig. 9** The face down (left) and end down (right) systems; the pentacene monomers in these systems are **a** (left) and **b** (right).

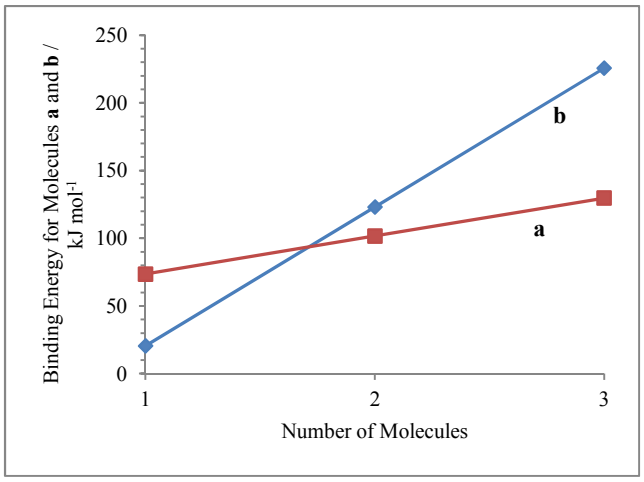


**Fig. 10** Binding energies for monomers **a** and **b** (see Fig. 9) as more molecules are added to the surface.

one can see that the binding energy for one molecule on a surface is greater for **a** than for **b**. As a second molecule is added, the binding energy for **b** surpasses that of **a**, since it is able to form a strongly bound face-to-face dimer. Once a third molecule has been added, the binding energy for **b** is significantly greater than the energy for **a**. This suggests that only two or three pentacene molecules must be interacting with one another before it is more favourable for them to stack in an upright configuration.



This journal is © The Royal Society of Chemistry [year]

Faraday Discussions Accepted Manuscript

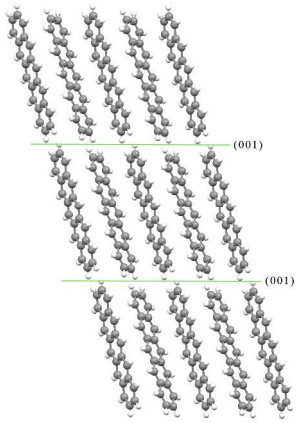


**Fig. 11** The (001) plane of crystalline pentacene.

**Orientation of Crystalline Clusters on the Surface.** Clusters of molecules were optimised on a silica surface in order to probe the morphology of a monolayer. The initial geometry was taken from the single crystal structure. In a pentacene monolayer, the (001) plane is in contact with the surface (Fig. 11). Taking a molecule on one side of a plane and calculating the binding energy to its nearest neighbour molecules on the other side, quantifies the interaction energy. This represents the loss of binding energy when the molecule is removed from the bulk onto the surface. This is akin to a molecular surface energy. Table 2 details the binding energy that would be missing for pentacene and TIPS-pentacene molecules if the crystal were 'cut' along planes which leave the ends, edges or faces of the molecules exposed.

**Table 2** The molecular surface energies along low energy planes for **1** and **2**.

| Molecule | Molecular Surface Energy / kJ mol$^{-1}$ | | |
|---|---|---|---|
| | End | Face | Edge |
| **1** | -26 | -214 | -153 |
| **2** | -209 | -276 | -60 |

The energy lost when the end of molecule **1** is left exposed is 26 kJ mol$^{-1}$ compared to 153 kJ mol$^{-1}$ for an edge; an almost five-fold increase. For **2**, the exposure of an edge is much more favourable than either of the other orientations. This data agrees and rationalises the known morphologies of **1** and **2** on the surface of amorphous silica.



This journal is © The Royal Society of Chemistry [year]

Faraday Discussions Accepted Manuscript

## Benzo[*k*]tetraphenes

The initial geometries on the surface were chosen by the procedure outlined above for pentacene. Table 3 below gives the planes identified and their binding energies.

**Table 3** The molecular surface energies along low energy planes for **3**, **4**, **5** and **6**.

| Structure | Plane | Molecular Surface Energy / kJ mol$^{-1}$ |
|---|---|---|
| **3** | (001) | -33 |
| | (0-21) | -122 |
| **4** | (001) | -33 |
| | (0-21) | -124 |
| **5** | (010) | -57 |
| | (100) | -119 |
| **6** | (100) | -142 |

For molecules **3**, **4** and to a slightly lesser extent, **5**, one plane of particularly low energy dominates in the crystal. For **6**, the lowest energy plane was found to be considerably larger in energy than any of the others in the set. In general, the bulky side groups tended to be exposed at the lowest energy planes.

## Optimisations

To model the morphology of a monolayer, a crystal fragment was placed on the surface, comprising of a central molecule and its nearest neighbours. The system was allowed to relax and the hole mobility for the resultant structure was calculated. In addition, hole mobilities of optimised crystal fragments were calculated. These provided a computational comparison for the surface optimisations. Unless stated otherwise, the crystal fragments consisted of a central molecule and its nearest neighbours.

Crystal fragment optimisations are dependent upon the number of molecules in the system. Molecules on the periphery, which are not fully saturated, have higher degrees of freedom than those in the centre. This means that smaller systems are poorer representations of the single crystal structure. However, computational limitations preclude the modelling of very large systems. For smaller molecules such as pentacene, with inherently fewer degrees of freedom than the functionalised cores, some analysis has been provided to indicate the differences between systems of varying size. A comparison for molecule **4** is given in order to investigate the effects of treating larger fragments on the geometries of the functionalised cores.

Hole mobilities can be rationalised by geometry changes from the crystal to the optimised structures. The parameters measured to quantify the geometries are the centroid-centroid distances between the central molecule and each of its nearest neighbours, and the angles between their planes (Fig. 12). In each



This journal is © The Royal Society of Chemistry [year]

Faraday Discussions Accepted Manuscript

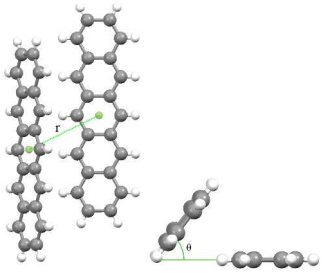


**Fig. 12** The centroid-centroid distance, *r*, between the central molecule and one of its nearest neighbours (left) and the angle between their planes, *θ*, (right).

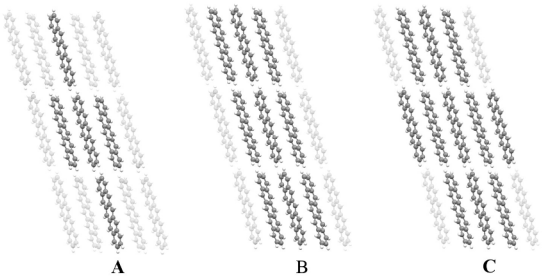


**Fig. 13** Systems of varying size for the fragment optimisation.

case, the averages in the differences of these parameters from the experimental to optimised cases have been evaluated to give an idea of the overall movement of a system.

**Fragment Optimisation**. Three differently sized systems were optimised for **1**, depicted in Fig. 13. For system **A**, only nearest neighbours were present; for system **B**, a few further stabilising molecules were inserted; and for system **C**, another molecular shell around the central molecules was included.

As the number of molecules in the system increases, there is a corresponding increase in the hole mobility. Comparing the values, we find that the mobility for the experimental crystal, **A** is approximately half, **B** is comparable to and **C** surpasses the mobility of the single crystal. The centroid-centroid distances differ from the experimental value on average between 0.4-0.6 Å and the angles change on average between 3.2-4.6°. This suggests that whilst the distances between the molecules vary during the optimisation, their angles remain roughly the same. This behaviour is shown distinctly in **C**, in which some of the molecules have moved considerably closer to the central molecule therefore increasing their electronic couplings and hence, the overall mobility.

**Monolayer Optimisation.** The monolayer optimisations comprise a central molecule and its nearest neighbours on the surface, shown in Fig. 14 for system **D**. To investigate the effect of the presence of more molecules in the optimisation, a calculation was run in which an additional molecular shell was added, shown in Fig. 14 as system **E**.



This journal is © The Royal Society of Chemistry [year]

Faraday Discussions Accepted Manuscript

**Fig. 14** Two pentacene monolayers; on the left is the smaller system containing only the nearest neighbours, **D**, and on the right is the larger system with an additional molecular shell around the central units, **E**.

For **D**, the mobility is approximately the same as the single crystal value. In **E**, a similar behaviour to **C** is observed as the molecules are compressed with little change in their angles. As a result, the hole mobility for **E** is much higher than for **D**; 6.8 $cm^2$ $V^{-1}$ $s^{-1}$. The hole mobilities for **C** and **E**, however, differ by approximately 3.6 $cm^2$ $V^{-1}$ $s^{-1}$. In the monolayer system, the electronic coupling value for one of the paths has increased. It is suspected that this behaviour has been effected by local variations in the structure of the surface, for instance whether a molecule resides above one of the middle of rings or over a group of atoms.

**Hole Mobilities**

**Table 4** Hole mobilities for all monomers in their single crystals, optimised fragments and monolayers, and their experimentally measured thin film mobilities.

| Molecule | Hole Mobility / $cm^2$ $V^{-1}$ $s^{-1}$ | | | | | |
|---|---|---|---|---|---|---|
| | Single Crystal | Optimised Fragment | | Optimised Monolayer | | Experimental Thin Film |
| **1** | 2.16 | **A** | 0.83 | **D** | 1.91 | >5[24] |
| | | **B** | 1.82 | | | |
| | | **C** | 3.20 | **E** | 6.85 | |
| **2** | 0.50 | | 0.05 | | 0.75 | 0.4[8] |
| **3** | 0.16 | | 2.84 | | 2.38 | 1.3 |
| **4** | 0.39 | **Small** | 3.36 | **Small** | 3.01 | 1.1 |
| | | **Large** | 1.87 | **Large** | 3.17 | |
| **5** | 0.20 | | 0.86 | | 0.47 | N/A |
| **6** | 0.44 | | 0.12 | | 0.77 | N/A |

Table 4 details the calculated mobilities for structures **1**-**6** along with their experimentally measured thin film mobilities, where available. The experimentally measured thin film mobilities were found to be poor. **5** and **6** formed amorphous thin films in which no field-effect mobility was observed. For **2**, the predicted mobility for the experimental structure is 0.50 $cm^2$ $V^{-1}$ $s^{-1}$. This value is dominated by two equivalent hopping paths with electronic coupling values of approximately 0.036 eV. In the optimised fragment, these couplings have reduced to approximately 0.007 eV. The major contributing factor is an increase in the displacement of the molecules' long axes. It is precisely the change in these coupling values, which has



This journal is © The Royal Society of Chemistry [year]

Faraday Discussions Accepted Manuscript

reduced the mobility for the optimised fragment by an order of magnitude.

For the optimised monolayer of **2**, the corresponding paths have electronic coupling values between 0.032 and 0.051 eV, which is similar to those in the experimental crystal structure. Since the rest of the electronic coupling values are larger for the optimised monolayer than the experimental crystal, the hole mobility is ~0.25 $cm^2 V^{-1} s^{-1}$ greater.

In their experimental crystal structures, **3** and **4** share the same packing motif, differing mainly in their centroid-centroid distances. For both cases, optimisation of the crystal fragment has led to a significant improvement in the hole mobility, due to large changes from the experimental structure. However, the centroid-centroid distances have reduced to a greater extent in the structure of **4** than in **3**, which is reflected in its higher hole mobility. This may be due to repulsion between F-atoms on neighbouring molecules in system **3**. The optimised fragment and monolayer share similar geometries, accounting for minimal differences in the mobility.

A further, larger fragment was taken for **4**, in order to investigate the effect of system size on the relaxation of the structures for the functionalised molecules. When more molecules are included in the optimisation, the hole mobility almost halves. Crucially, some of the centroid-centroid distances increase with respect to the experimental structure, reducing the electronic coupling values and consequently, the overall mobility. Interestingly, for the monolayer optimisation of **4**, the mobility changes little on increasing the number of molecules in the system. The geometries however, are quite different.

For structure **5**, there is a four-fold increase in the mobility for the optimised fragment compared with the experimental crystal, due to significant differences in geometry. In fact, some of the changes during the optimisation would be unphysical in the actual crystal environment. For the optimised monolayer of **5**, the structure is again significantly different from the experimental crystal, with some larger and some smaller centroid-centroid distances. Overall, more of the hopping paths have electronic coupling values that are larger in the optimised monolayer than the crystal, which has led to a two-fold increase in the hole mobility. The mobilities for both the fragment and monolayer optimisations are not as high as the corresponding mobilities for structures **3** and **4**. The larger substituents in structure **5** preclude shorter distances between molecules due to steric hindrance.

The single crystal packing motif for **6** differs from the other structures in this series, a change that may be caused by the larger size of the substituent. A decrease in the hole mobility compared with the single crystal has been found for optimisation of the crystal fragment. This is likely due to changes in the relative orientations of the molecules. Following optimisation of the monolayer, the hole mobility is almost double that of the single crystal. The intermolecular distance in the starting geometry is significantly greater than in the optimised structure. The average change in the centroid-centroid distances for the molecules is 2.92 Å. In addition, the angles between molecular planes are altered on average by 42.1°. Overall, this optimisation represents a case in which there is such significant reorganisation of the structure such that it no longer resembles the initial geometry. This may be related to the likelihood of formation of an amorphous film.

The hole mobilities for molecules **3** and **4**, which have similar structures, have significantly increased post-optimisation. On the other hand, the mobilities for molecules **5** and **6** have changed more modestly. This indicates a correlation between the size of the substituent and the ability for the structure to reorganise in



This journal is © The Royal Society of Chemistry [year]

Faraday Discussions Accepted Manuscript

such a way that increases the mobility.

## 3 Conclusions

It has been shown in this investigation that optimisation of a structure on a surface can significantly affect the predicted hole mobility. Structures **3** and **4** have relatively low predicted mobility values in the single crystal phase compared with those for the optimised monolayers. This is in accord with experimental observation. The calculations using different sized fragments suggest that more molecules must be incorporated to obtain accurate hole mobilities.

As a further refinement of the model, different surface structures should be investigated. This would enable the study of any surface modifications on the mobility.

## Acknowledgement

R. A. K. thanks The University of Manchester Alumni Fund for the award of a Research Impact Scholarship and Merck Chemicals Ltd. for financial support.

## References

[a] *School of Chemistry, The University of Manchester, Manchester, M13 9PL, UK.; E-mail: rose.krawczuk@postgrad.manchester.ac.uk.*
[b] *Merck Chemicals Ltd., Chilworth Technical Centre, University Parkway, Southampton, SO16 7QD, UK.*

1 B. Kumar, B. K. Kaushik and Y. S. Negi, *Polymer Rev*., 2014, **54**, 33.
2 D. Choudhary, P. Clancy, R. Shetty and F. Escobedo, *Adv. Funct. Mater*., 2006, **16**, 1768.
3 J. E. Anthony, J. S. Brooks, D. L. Eaton and S. R. Parkin, *J. Am. Chem. Soc*., 2001, **123**, 9482.
4 S. Chen and J. Ma, *J. Chem. Phys*., 2012, **137**, 074708.
5 7. C. Kim and D. Jeon, *Ultramicroscopy*, 2008, **108**, 1050.
6 S. E. Fritz, S. M. Martin, C. D. Frisbie, M. D. Ward and M. F. Toney, *J. Am. Chem. Soc*., 2004, **126**, 4084.
7 S. C. B. Mannsfeld, A. Virkar, C. Reese, M. F. Toney and Z. Bao, *Adv. Mater*., 2009, **21**, 2294.
8 S. C. B. Mannsfeld, M. L. Tang and Z. Bao, *Adv. Mater*., 2011, **23**, 127.
9 F.-J. Meyer zu Heringdorf, M. C. Ruter and B. M. Tromp, *Nature*, 2001, **412**, 517.
10 R. G. Della Valle, E. Venuti, A. Brillante and A. Girlando, *ChemPhysChem*, 2009, **10**, 1783.
11 L. Viani, C. Risko, M. F. Toney, D. W. Breiby and J.-L. Brédas, *ACS Nano*, 2014, **8**, 690.
12 P. Clancy, *Chem. Mater.*, 2011, **23**, 522.
13 J. Veres, S. Ogier, G. Lloyd and D. de Leeuw, *Chem. Mater.*, 2004, **16**, 4543.
14 D. Knipp, R. A. Street, A. Volkel and J. Ho, *J. Appl. Phys.*, 2003, **93**, 347.
15 S. A. DiBenedetto, A. Facchetti, M. A. Ratner and T. J. Marks, *Adv. Mater*., 2009, **21**, 1407.
16 J. E. McDermott, M. McDowell, I. G. Hill, J. Hwang, A. Kahn, S. L. Bernasek and J. Schwartz, *J. Phys. Chem. A*, 2007, **111**, 12333.
17 E. F. Valeev, V. Coropceanu, D. A. da Silva Filho, S. Salman and J.-L. Brédas, *J. Am. Chem. Soc*., 2006, **128**, 9882.
18 H. T. Nicolai, M. Kuik, G. A. H. Wetzelaer, B. de Boer, C. Campbell, C. Risko, J. L. Brédas and P. W. M. Blom, *Nature Mater*., 2012, **11**, 882.
19 A. Rimola, B. Civalleri and P. Ugliengo, *Phys. Chem. Chem. Phys*., 2010, **12**, 6357.
20 *Wo. Pat.*, WO2012076092A1, 2012.
21 (a) MOPAC2012, J. J. P. Stewart, Stewart Computational Chemistry, Version 13.313L.
(b) J. D. C. Maia, G. A. Urquiza Carvalho, C. P. Mangueira, S. R. Santana, L. A. F. Cabral and G. B. Rocha, *J. Chem. Theory Comput*., 2012, **8**, 3072.
22 (a) A. D. Becke, *J. Chem. Phys*., 1993, 98, 5648-52.



This journal is © The Royal Society of Chemistry [year]

Faraday Discussions Accepted Manuscript

(b) C. Lee, W. Yang and R. G. Parr, *Phys. Rev. B*, 1988, **37**, 785-89.
(c) B. Miehlich, A. Savin, H. Stoll and H. Preuss, *Chem. Phys. Lett*., 1989, **157**, 200.
23 Gaussian 09, Revision D.01, M. J. Frisch, G. W. Trucks, H. B. Schlegel, G. E. Scuseria, M. A. Robb, J. R. Cheeseman, G. Scalmani, V. Barone, B. Mennucci, G. A. Petersson, H. Nakatsuji, M. Caricato, X. Li, H. P. Hratchian, A. F. Izmaylov, J. Bloino, G. Zheng, J. L. Sonnenberg, M. Hada, M. Ehara, K. Toyota, R. Fukuda, J. Hasegawa, M. Ishida, T. Nakajima, Y. Honda, O. Kitao, H. Nakai, T. Vreven, J. A. Montgomery, Jr., J. E. Peralta, F. Ogliaro, M. Bearpark, J. J. Heyd, E. Brothers, K. N. Kudin, V. N. Staroverov, R. Kobayashi, J. Normand, K. Raghavachari, A. Rendell, J. C. Burant, S. S. Iyengar, J. Tomasi, M. Cossi, N. Rega, J. M. Millam, M. Klene, J. E. Knox, J. B. Cross, V. Bakken, C. Adamo, J. Jaramillo, R. Gomperts, R. E. Stratmann, O. Yazyev, A. J. Austin, R. Cammi, C. Pomelli, J. W. Ochterski, R. L. Martin, K. Morokuma, V. G. Zakrzewski, G. A. Voth, P. Salvador, J. J. Dannenberg, S. Dapprich, A. D. Daniels, Ö. Farkas, J. B. Foresman, J. V. Ortiz, J. Cioslowski and D. J. Fox, Gaussian, Inc., Wallingford CT, 2009.
24 T. W. Kelley, P. F. Baude, C. Gerlach, D. E. Ender, D. Muyres, M. A. Haase, D. E. Vogel and S. D. Theiss, *Chem. Mater*., 2004, **16**, 4413.



This journal is © The Royal Society of Chemistry [year]

Faraday Discussions Accepted Manuscript